Full-wave Analysis of Aperture Coupled Shielded Microstrip Lines

N. L. VandenBerg and P. B. Katehi

Radiation Laboratory, The University of Michigan, Ann Arbor, MI

Abstract

A full-wave space-domain integral equation analysis of aperture coupled shielded microstrip lines is presented based on Pocklington's integrals and the equivalence principle. The derivation of the associated dyadic Green's functions in the form of waveguide LSE and LSM modes is described. The line currents and slot voltage are expanded in terms of subsectional basis functions and the method of moments, together with even and odd mode transmission line analysis, is applied to determine the two-port scattering parameters. A particular case is illustrated which demonstrates the behavior of the coupler as a bandpass interconnect.

Introduction

Application of monolithic techniques to microwave and millimeter-wave circuits has introduced the need for accurate full-wave analysis to account for the effects of the shielding structure and also the interaction of circuit elements which may be closely spaced. These effects may not be accounted for by other methods such as simple transmission line analysis, especially as frequency increases. Additionally, high-frequency interconnect approaches are required which must be accurately modeled for design and also must fit well in a monolithic fabrication scheme.

Transitions from microstrip to slotline have long been recognized as important circuit elements. Numerous investigators have presented approximate analytical techniques to characterize these structures with applications to circuit elements [1] - [4]. A full-wave analysis for this transition was reported in [5] with applications to open structures.

In this paper, the analysis of aperture coupled shielded microstrip lines is presented. This structure, in a variety of forms, has a wide range of applications to both broadband and narrowband connections and can be used as a building block for interconnects [6], phase shifters and inverters [7], directional couplers [8] as well as filters. A quasi-static analysis has been provided in [9], however, this may not be sufficient, particularly for higher frequencies where end effects and higher order mode coupling become more significant. A more recent paper [10] presents a transmission line analysis with excellent results, however, similar shortcomings would be expected. Hybrid methods which combine two-dimensional full-wave analysis with transmission line theory, as in [11], should certainly extend the validity of such models, however, may still not account for all discontinuity effects. Our approach uses a three-dimensional full-wave space-domain integral equation method employing the method of moments with Galerkin's procedure to account for all possible interactions.

Analysis

The basic structure of the coupler to be discussed is as shown in Figure 1. Variations on this geometry include cases where the strips are on the same substrate in a single cavity, addition of multiple layers to the substrates/superstrates, reverse couplers where the lines exit on the same wall, parallel slots and lines, among others, but can all be analyzed using the same approach.

The analysis proceeds as follows: the slot is replaced on both sides by an equivalent magnetic current – representing the tangential electric field in the slot – backed by a perfectly conducting wall (all walls will be assumed to be perfect conductors). In this case, the problem is now separated into two independent regions, coupled together by the magnetic current. Using the same current on either side enforces the continuity of the electric field in the slot. The fields in the cavities can now be written in term's of Pocklington integrals as follows:

$$\overline{\mathrm{E}} = -j\omega\mu \iint \bar{\bar{\mathrm{G}}}_{\mathrm{eJ}} \cdot \bar{\mathrm{J}}\ dS' - \iint \bar{\bar{\mathrm{G}}}_{\mathrm{eK}} \cdot \overline{\mathrm{K}}\ dS' \quad (1)$$

$$\overline{\mathrm{H}} = \iint \bar{\bar{\mathrm{G}}}_{\mathrm{mJ}} \cdot \bar{\mathrm{J}}\ dS' - j\omega\epsilon \iint \bar{\bar{\mathrm{G}}}_{\mathrm{mK}} \cdot \overline{\mathrm{K}}\ dS' \quad (2)$$

The subscripts on the Green's functions indicate whether the function is of the electric (e) or magnetic (m) field type for electric (J) or magnetic (K) currents.

By using the appropriate rectangular cavity Green's functions, the fields in the cavities satisfy the boundary conditions on the walls. The remaining boundary conditions, zero tangential electric field on the strips and continuous tangential magnetic field in the slot, allow us to write the integral equations which are

$$-j\omega\mu \iint_{strip_L} \bar{\bar{G}}_{eJ}^{strip_L} \cdot \bar{J}_L \, dS' - \iint_{slot} \bar{\bar{G}}_{eK}^{strip_L} \cdot \overline{K} dS'' = 0^* \quad (3)$$

$$\iint_{strip_L} \bar{\bar{G}}_{mJ}^{slot} \cdot \bar{J}_L \, dS' - j\omega \iint_{slot} \left[\epsilon_L \bar{\bar{G}}_{mK}^{slot} + \epsilon_U \bar{\bar{G}}_{mK}^{slot} \right] \cdot \overline{K} dS'' - \iint_{strip_U} \bar{\bar{G}}_{mJ}^{slot} \cdot \bar{J}_U \, dS' = 0 \quad (4)$$

$$\iint_{slot} \bar{\bar{G}}_{eK}^{strip_U} \cdot \overline{K} dS'' - j\omega\mu \iint_{strip_U} \bar{\bar{G}}_{eJ}^{strip_U} \cdot \bar{J}_U \, dS' = 0^* \quad (5)$$

where 0^* implies that the field is non-zero at gap generator locations. The superscript indicates the evaluation point for the field.

The Green's functions are solutions to the dyadic equations:

$$\nabla \times \nabla \times \bar{\bar{G}}_{eJ} - k^2 \bar{\bar{G}}_{eJ} = \bar{\bar{I}} \delta(\bar{R} - \bar{R}') \quad (6)$$

$$\nabla \times \nabla \times \bar{\bar{G}}_{mJ} - k^2 \bar{\bar{G}}_{mJ} = \nabla \times [\bar{\bar{I}} \delta(\bar{R} - \bar{R}')] \quad (7)$$

$$\nabla \times \nabla \times \bar{\bar{G}}_{mK} - k^2 \bar{\bar{G}}_{mK} = \bar{\bar{I}} \delta(\bar{R} - \bar{R}') \quad (8)$$

$$\nabla \times \nabla \times \bar{\bar{G}}_{eK} - k^2 \bar{\bar{G}}_{eK} = \nabla \times \bar{\bar{I}} \delta(\bar{R} - \bar{R}') \quad (9)$$

Solutions to these equations can be found for geometries of the type illustrated in Figure 2 where the impedance boundary conditions allow for treatment of multi-layered substrates and superstrates as may be encountered in monolithic circuits. The Green's function is found for the layer containing the strips or slot by applying transmission line theory to the other layers to obtain the impedance boundary conditions (η) corresponding to each mode. Subsequently, the fields in the other layers can be found from the homogeneous solutions to Equations (6 - 9) and a pair of coupling coefficients for each layer. The solutions are expanded in terms of LSE and LSM modes which facilitates finding the fields in the remaining layers since these modes are decoupled on the boundaries and can be individually matched to like modes in adjacent layers. The coupling coefficients are then readily found by matching the tangential field components at successive layers.

The longitudinal current components are now expanded in terms of piecewise sinusoidal functions with a Maxwellian transverse distribution which satisfies the edge conditions. In general, the currents are written in terms of both longitudinal and transverse components however, in this case, it will be assumed that both the slot and the strips are narrow enough so that the longitudinal components of current dominate their behavior and the transverse components can be neglected. The integral equations can now be written as a matrix equation in conventional method of moments fashion.

The inverted matrix is then used with even and odd gap generator excitations at the line ends to find the currents on the microstrip lines. From the even and odd currents, the scattering parameters can be found which characterize the coupling behavior.

Numerical Results

A coupler with the geometry of Figure 1 was analyzed using the above techniques. The parameters which can be varied in this design are numerous, consequently, only a few variations will be presented here. In all cases, although not required in general, symmetric geometry is maintained to simplify the even and odd mode analysis.

Figures 3 – 4 illustrate the affect of the line stub lengths (l – see Figure 1) on the coupling coefficients. Variation of these lengths has the effect of changing the position of the current maxima (virtual shorts) on the lines relative to the slot, thus varying the degree of coupling through the slot. Also shown is the affect of the line separation parameter (s) on the coupling behavior. Note the increase in phase shift due to the added length of slotline as the separation is increased.

The affect of the slot length is shown in Figure 5. Using a transmission line analogy, one can interpret this effect by transforming the impedances at the ends of the slot to the center, which demonstrates that as the slot becomes very short, the field in the slot is effectively "short circuited", thus coupling is reduced. This effect would be expected to repeat as the slot length increases in multiples of λ, however, for the case studied here, the maximum slot length is limited by the dimensions of the shielding package (.25 × .25 inches) which are chosen to allow only the dominant microstrip mode to propagate. As the length of the slot approaches zero, S_{21} tends to zero while S_{11} approaches unity (since the structure is closed). The phase of S_{11} referenced to the end of the line becomes the phase due to the end effect, typically, -10 to -15 degrees.

The frequency response shown in Figure 6 demonstrates the utility of the structure as a filter. With proper selection of the geometric parameters such as line and slot widths, line separation and substrate heights, the frequency response can be tailored to give the required center frequency, bandwidth, shape, etc. In the case studied here, the length of the lines were fixed at .725 inches which corresponds to line stub lengths of approximately $3\lambda/8$ at 12 GHz which was the frequency for Figures 3 – 5. Also, the width of the slot was the same as the line width (.025 inches on $\epsilon_r = 9.7$, $W/h = 1$ substrate) which results in a microstrip-to-slotline characteristic impedance mismatch of more than $2:1$. As expected under these conditions, the bandwidth is much narrower than in [10] where better than octave performance is demonstrated. Matching the slot impedance and modifying the width of the stubs as in [10] can be readily accomplished with this method to analyze broadband interconnects.

Unfortunately, because the slot length for this simple geometry is typically on the order of $\lambda/2$ to get low loss coupling, it may not represent a good choice for monolithic integrated circuit applications where small size is required. Therefore, future analytical and experimental efforts are planned to study and optimize the performance/size tradeoffs for this class of couplers while taking full advantage of the benefits of full-wave analysis for high frequency applications. For example, it may be possible to introduce combinations of shorter slots of varying lengths to produce a broadband frequency response while maintaining a reasonably small area of chip real estate.

Conclusions

A set of integral equations for aperture coupled shielded microstrip lines has been introduced based on Pocklington's integrals and the equivalence principle. The associated dyadic Green's functions in the form of waveguide LSE and LSM modes have been derived which allow for a full-wave analysis, accounting for all electromagnetic interactions of a microstrip – slot coupler. By expanding the unknown line currents and slot voltage in terms of subsectional basis functions and applying the method of moments together with even and odd mode transmission line analysis, the two-port scattering coefficients can be determined. The method has been applied to a particular case which demonstrates the behavior of the coupler as a bandpass interconnect.

Acknowledgement

This work was supported by the *National Science Foundation* under contract ECS:8657951 and partially by the *NASA Center for Space Terahertz Technology* .

References

[1] S. B. Cohn, "Slot line on a dielectric substrate." *IEEE Transactions on Microwave Theory and Techniques*, Vol. MTT-17, No. 10, October 1969, pp. 768-778.

[2] E. A. Mariani, C. P. Heinzman, J. P. Agrios and S. B. Cohn, "Slot line characteristics." *IEEE Transactions on Microwave Theory and Techniques*, Vol. MTT-17, No. 12, December 1969, pp. 1091-1096.

[3] E. A. Mariani and J. P. Agrios, "Slot-line filters and couplers." *IEEE Transactions on Microwave Theory and Techniques*, Vol. MTT-18, No. 12, December 1970, pp. 1089-1095.

[4] J. B. Knorr, "Slot-line transitions." *IEEE Transactions on Microwave Theory and Techniques*, Vol. MTT-22, No. 5, May 1974, pp. 548-554.

[5] H. Yang and N. G. Alexopoulos, "A dynamic model for microstrip-slotline transition and related structures." *IEEE Transactions on Microwave Theory and Techniques*, Vol. MTT-36, No. 2, February 1988, pp. 286-293.

[6] R. H. Jansen, R. G. Arnold and I. G. Eddison, "A comprehensive CAD approach to the design of MMIC's up to MM-wave frequencies." *IEEE Transactions on Microwave Theory and Techniques*, Vol. MTT-36, No. 2, February 1988, pp. 208-219.

[7] K. G. Gupta, R. Garg and I. J. Bahl, *Microstrip Lines and Slotlines*, Artech House, Dedham, MA, 1979.

[8] T. Tanaka, K. Tsunoda and M Aikawa, "Slot-coupled directional couplers between double-sided substrate microstrip lines and their applications." *IEEE Transactions on Microwave Theory and Techniques*, Vol. MTT-36, No. 12, December 1988, pp. 1752-1757.

[9] S. Yamamoto, T. Azakami and K. Itakura, "Slit-coupled strip transmission lines." *IEEE Transactions on Microwave Theory and Techniques*, Vol. MTT-14, No. 11, November 1966, pp. 542-553.

[10] B. Schüppert, "Microstrip/slotline transitions: Modeling and experimental investigation." *IEEE Transactions on Microwave Theory and Techniques*, Vol. MTT-36, No. 8, August 1988, pp. 1272-1282.

[11] H. Ogawa, T. Hirota and M. Aikawa, "New MIC power dividers using coupled microstrip-slot lines: Two-sided MIC power dividers." *IEEE Transactions on Microwave Theory and Techniques*, Vol. MTT-33, No. 11, November 1985, pp. 1155-1164.

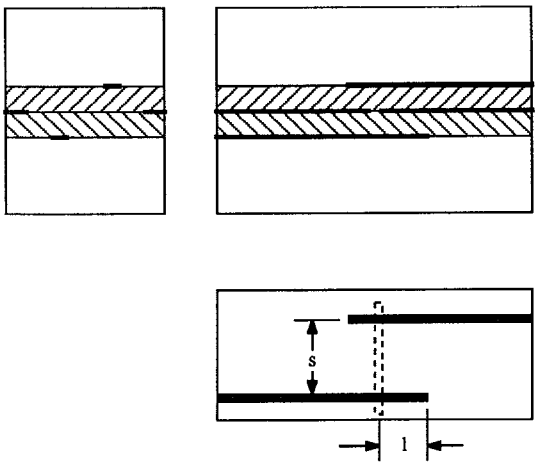

Figure 1: Geometry of basic coupler.

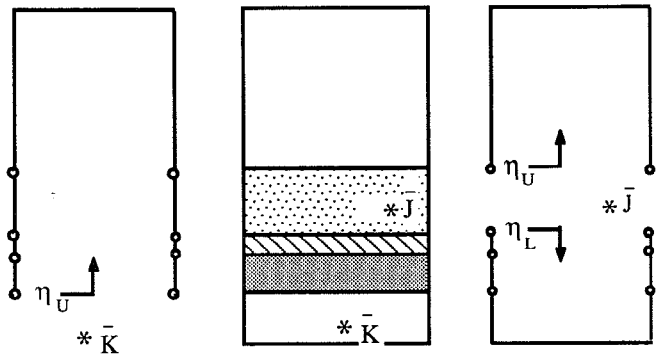

Figure 2: Sample multi-layered structure.

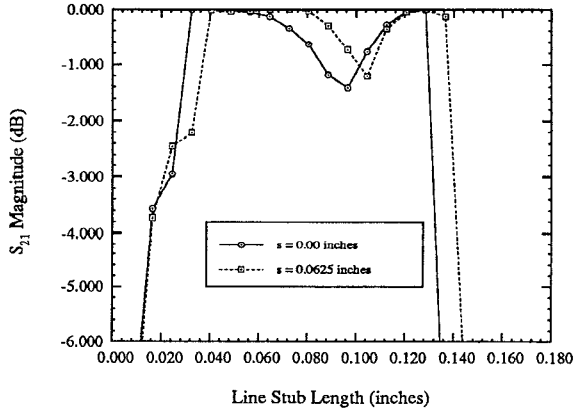

Figure 3: Variation of S_{21} magnitude with line stub lengths.

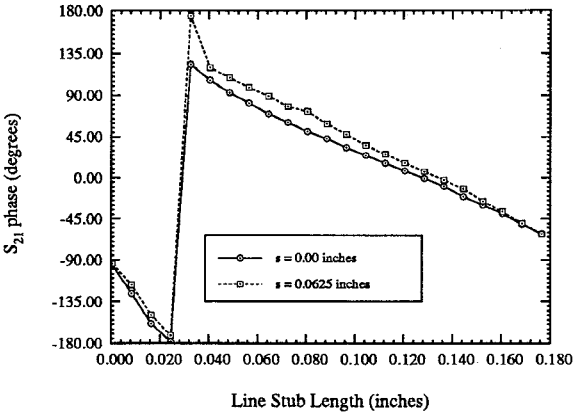

Figure 4: Variation of S_{21} phase with line stub lengths.

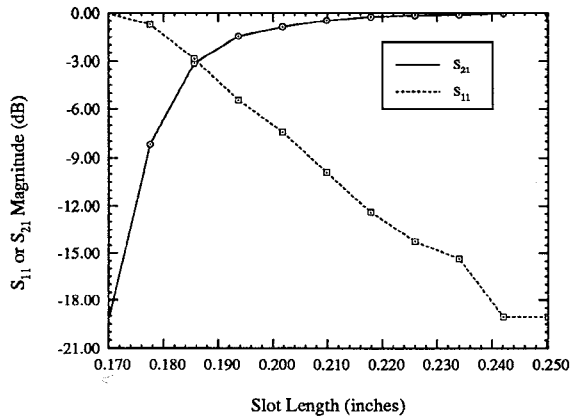

Figure 5: Affect of slot length on S_{21} and S_{11} magnitudes.

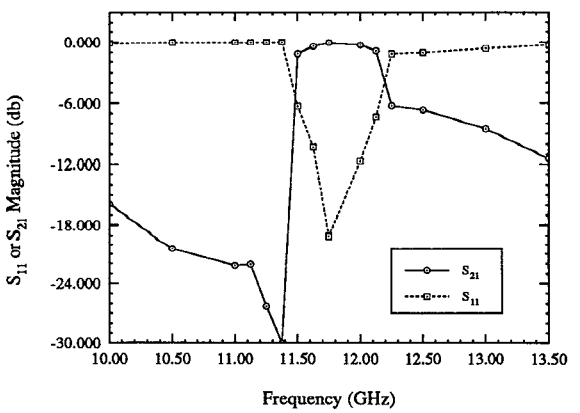

Figure 6: Coupler frequency response.